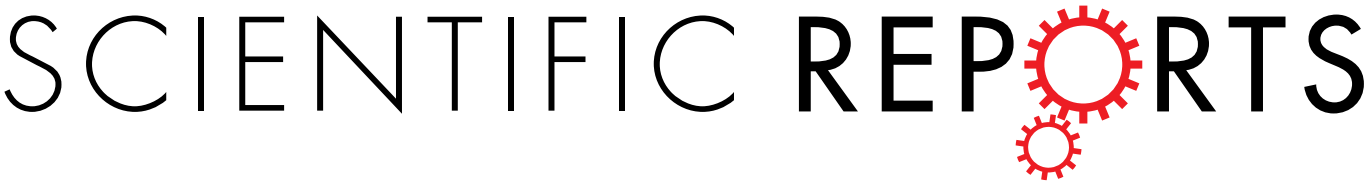

OPEN

Tunable Bistability in Hybrid Bose-Einstein Condensate Optomechanics

Received: 24 December 2014
Accepted: 21 April 2015
Published: 02 June 2015

Kashif Ammar Yasir & Wu-Ming Liu

Cavity-optomechanics, a rapidly developing area of research, has made a remarkable progress. A stunning manifestation of optomechanical phenomena is in exploiting the mechanical effects of light to couple the optical degree of freedom with mechanical degree of freedom. In this report, we investigate the controlled bistable dynamics of such hybrid optomechanical system composed of cigar-shaped Bose-Einstein condensate (BEC) trapped inside high-finesse optical cavity with one moving-end mirror and is driven by a single mode optical field. The numerical results provide evidence for controlled optical bistability in optomechanics using transverse optical field which directly interacts with atoms causing the coupling of transverse field with momentum side modes, exited by intra-cavity field. This technique of transverse field coupling is also used to control bistable dynamics of both moving-end mirror and BEC. The report provides an understanding of temporal dynamics of moving-end mirror and BEC with respect to transverse field. Moreover, dependence of effective potential of the system on transverse field has also been discussed. To observe this phenomena in laboratory, we have suggested a certain set of experimental parameters. These findings provide a platform to investigate the tunable behavior of novel phenomenon like electromagnetically induced transparency and entanglement in hybrid systems.

In last few years, a lot of investigations have been conducted in the field of cavity-optomechanics. Experimental advances in cavity-optomechanics have made it possible to couple mechanical resonator with optical degree of freedom[1]. Another milestone was achieved by the demonstration of optomechanics when other physical objects, most notably cold atoms or Bose-Einstein condensate, were trapped inside cavity-optomechanics[2]. Both mirror-field interaction and atom-field interaction are needed to develop numerous sensors and devices in quantum metrology, and to study both these phenomena, we rely on hybrid optomechanical systems. In optomechanics, the movable mirror can be cooled down, by the mechanical effects of light, to its quantum mechanical ground state[3–7], thus providing a platform to study strong coupling effects in hybrid systems[8–11]. Such extraordinary investigaions in opto-mechanics motivate researchers in developing gravitational wave detectors[12], measuring displacement with large accuracy[13] and also in developing optomechanical crystals[14]. Recent discussion on bistable behaviour of BEC-optomechanical system[15], high fidelity state transfer[16,17], entanglement in optomechanics[18–21], macroscopic tunneling of an optomechanical membrane[22] and role reversal between matter-wave and quantized light field, are directing and facilitating researchers towards achieving new mile-stones in cavity-optomechanics. Furthermore, the magnificent work on transparency in optomechanics[23–26], dynamical localization in field of cavity-optomechanics[27,28] and the coupled arrays of micro-cavities[29–32] provide clear understanding for cavity-optomechanics. These notable achievements provide strong foundations to study complex systems and cause curiosity among researchers to explore such hybrid systems and so, a lot of work has been done in this regard[33–37].

Beijing National Laboratory for Condensed Matter Physics, Institute of Physics, Chinese Academy of Sciences, Beijing 100190, China. Correspondence and requests for materials should be addressed to K.A.Y. (email: kashif_ammar@yahoo.com) or W-M.L. (email: wliu@iphy.ac.cn)

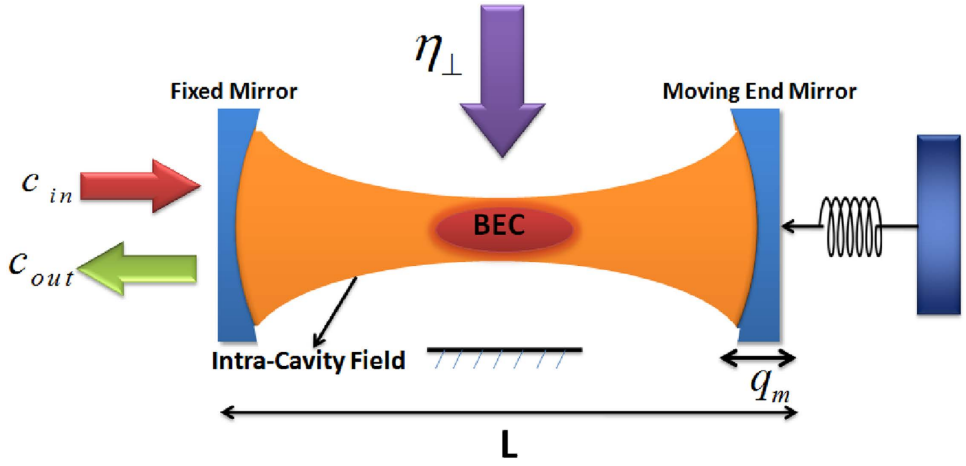

Figure 1. The hybrid BEC-Optomechanics. Cigar-shaped Bose-Einstein condensate is trapped inside a Fabry-Pérot cavity of length L with a fixed mirror and a moving-end mirror having maximum amplitude of q_0 and frequency ω_m, driven by a single mode optical field with frequency ω_p. Intra-cavity field interacts with BEC and due to photon recoil, the momentum side modes are generated in the matter wave. We use another transverse field, with intensity $\eta_\perp$ and frequency $\omega_\perp$, to control the bistable dynamics of the system.

In this report, we investigate tunable bistable behavior of optomechanical system which consists of one fixed mirror, one moving-end mirror with maximum amplitude q_0[1] and Bose-Einstein condensate (BEC) trapped inside the cavity, driven by a single mode optical field[38,39]. The idea of present work is motivated by the findings of Ref. 39. They demonstrated controlled optical switching of field inside an optical cavity containing ultra-cold atoms. They used transverse optical field to control bistable behavior of intra-cavity photons induced by external pump field. We use this approach of transverse optical field to control the bistable behavior of hybrid optomechanical system and show that the optical bistability or photons bistability inside the cavity is increased by increasing the strength of transverse field. The demonstration of results shows that the transverse optical field can also be used to control the bistable dynamics of moving-end mirror as well as BEC. We also investigate how this bistable behavior can affect the effective potential of the system. The set of experimental parameters which make these results experimentally feasible in laboratory has also been provided.

BEC Optomechanics

Optomechanical system which is a Fabry-Pérot cavity of length L consists of a fixed mirror and a moving-end mirror driven by a single mode parallel pump field with frequency ω_p, as shown in Fig. 1. Cigar-Shaped BEC, with N-two level atoms, is trapped inside optical cavity[2,40,41]. Moreover, optomechanical system is also driven by transverse optical field which interacts perpendicularly with BEC with intensity $\eta_\perp$ and frequency $\omega_\perp$[38,39,42]. Counter propagating field inside the cavity forms a one-dimensional optical lattice. The moving-end mirror possesses harmonic vibrations under radiation pressure with frequency ω_m, with maximum amplitude q_0 and exhibits Brownian motion in the absence of intra-cavity field. To make this study of tunable bistability in hybrid BEC-Optomechanics experimentally feasible, we suggest a set of particular parameters from present available experimental setups[1,2,41,43,44]. We consider $N = 2.3 \times 4\ ^{87}Rb$ atoms trapped inside Fabry-Pérot cavity with length $L = 1.25 \times 10^{-4}$, driven by single mode external field with power $P_{in} = 0.0164mW$, frequency $\omega_p = 3.8 \times 2\pi \times 10^{14}\,Hz$ and wavelength $\lambda_p = 780nm$. The frequency of intra-cavity field is $\omega_c = 15.3 \times 2\pi \times 10^{14}\,Hz$, with decay rate $\kappa = 1.3 \times 2\pi kHz$. Intra-cavity field produces recoil of $\omega_r = 3.8 \times 2\pi kHz$ in atoms trapped inside cavity. Intra-cavity atomic mode performs harmonic motion with damping rate $\gamma_a = 0.21 \times 2\pi kHz$. The coupling of intra-cavity field with BEC is $\xi_{sm} = 4.4\,MHz$. Detuning of the system is taken as $\Delta = \Delta_c + U_0 N/2 = 0.52 \times 2\pi MHz$, where vacuum Rabi frequency of the system is $U_0 = 3.1 \times 2\pi MHz$. The moving-end mirror of cavity should be a perfect reflector that oscillates with a frequency $\omega_m = 15.2 \times 2\pi MHz$ and damping $\gamma_m = 1.1 \times 2\pi kHz$. strength of its coupling with intra-cavity field is considered as $\xi = 3.8\,MHz$.

The complete Hamiltonian of the system consists of three parts,

$$\hat{H} = \hat{H}_{AF} + \hat{H}_{MF} + \hat{H}_T, \tag{1}$$

where, $\hat{H}_{AF}$ describes behavior of the atomic mode (BEC) and its coupling with cavity-optomechanics, $\hat{H}_{MF}$ is related to the intra-cavity field and its association with the moving-end mirror while, $\hat{H}_T$ accounts for noises and damping associated with the system.

We use strong detuning regime to adiabatically eliminate internal excited levels of atomic mode inside the cavity potential. We further apply rotating frame at external field frequency to derive Hamiltonian H_{AF} having quantized motion of atoms along the cavity axis. To avoid atom-atom interactions in BEC, we assume BEC is dilute enough so that many-body interaction effects can easily be ignored[38,39].

$$\hat{H}_{AF} = \int \hat{\psi}^{\dagger}(x)\left(-\frac{\hbar d^2}{2m_a dx^2} + \hbar U_0 \hat{c}^{\dagger}\hat{c}\cos^2 kx + \eta_{\perp} cos\,(kx)\,(\hat{c}^{\dagger} + \hat{c})\right)\hat{\psi}(x)\,dx, \tag{2}$$

$\hat{\psi}\left(\hat{\psi}^{\dagger}\right)$ is bosonic annihilation (creation) operator and $U_0 = g_0^2/\Delta_a$, g_0 is the vacuum Rabi frequency and Δ_a is far-off detuning between field frequency and atomic transition frequency ω_0. The mass of an atom is represented by m_a and k is the wave number for intra-cavity field. $\eta_{\perp} = g_0\Omega_p/\Delta_a$ is the coupling of BEC with transverse field and represents maximum scattering and Ω_p is the Rabi frequency of the transverse pump field. Due to field interaction with BEC, photon recoil takes place that generates symmetric momentum $\pm 2l\hbar k$ side modes, where, l is an integer. In the presence of weak field approximation, we consider low photon coupling. Therefore, only lowest order perturbation of the wave function will survive and higher order perturbation will be ignored. So, $\hat{\psi}$ is defined depending upon these 0^{th}, 1^{st} and 2^{nd} modes[15] as,

$$\hat{\psi}(x) = \frac{1}{\sqrt{L}}[\hat{b}_0 + \sqrt{2}\,cos\,(kx)\,\hat{b}_1 + \sqrt{2}\,cos\,(2kx)\,\hat{b}_2] \tag{3}$$

here, $\hat{b}_0$, $\hat{b}_1$ and $\hat{b}_2$ are annihilation operators for 0^{th} , 1^{st} and 2^{nd} modes respectively. By using $\hat{\psi}(x)$ defined above in Hamiltonian H_a, we write the Hamiltonian governing the field-condensate interaction as,

$$\hat{H}_{AF} = \omega_r \hat{b}_1^{\dagger}\hat{b}_1 + 4\omega_r \hat{b}_2^{\dagger}\hat{b}_2 + \frac{U_0}{4}\hat{c}^{\dagger}\hat{c}\left[\sqrt{2}\left(\hat{b}_0^{\dagger}\hat{b}_2 + \hat{b}_2^{\dagger}\hat{b}_0\right) + 2N + \hat{b}_1^{\dagger}\hat{b}_1\right]$$

$$+\frac{\eta_{\perp}}{2}(\hat{c}^{\dagger} + \hat{c})\left[\sqrt{2}\left(\hat{b}_0^{\dagger}\hat{b}_1 + \omega_r \hat{b}_1^{\dagger}\hat{b}_0\right) + \left(\hat{b}_1^{\dagger}\hat{b}_2 + \hat{b}_2^{\dagger}\hat{b}_1\right)\right]. \tag{4}$$

The sum of number of particles in all momentum side modes is, $\hat{b}_0^{\dagger}\hat{b}_0 + \hat{b}_1^{\dagger}\hat{b}_1 + \hat{b}_2^{\dagger}\hat{b}_2 = N$, where, N is the total number of bosonic particles. As population in 0^{th} mode is much larger than the population in 1^{st} and 2^{nd} order side mode, therefore, we can comparatively ignore the population in 1^{st} and 2^{nd} order side mode and can write $\hat{b}_0^{\dagger}\hat{b}_0 \simeq N$ or $\hat{b}_0$ and $\hat{b}_0^{\dagger} \rightarrow \sqrt{N}$. This is possible when side modes are weak enough to be ignored. Under these assumptions, we write simplified form of BEC-field Hamiltonian,

$$\hat{H}_{AF} = \frac{\hbar U_0 N}{2}\hat{c}^{\dagger}\hat{c} + \frac{\hbar\Omega}{2}\left(\hat{P}^2 + \hat{Q}^2\right) + \xi_{sm}\hbar\hat{c}^{\dagger}\hat{c}\hat{Q} + \hbar\eta_{eff}\hat{Q}(\hat{c}^{\dagger} + \hat{c}). \tag{5}$$

First term accommodates the effects of condensate on intra-cavity field and Δ_a is the atom-field detuning. Second term describes the motion of condensate inside the cavity. $\hat{P} = \frac{i}{\sqrt{2}}\left(\hat{b} - \hat{b}^{\dagger}\right)$ and $\hat{Q} = \frac{1}{\sqrt{2}}\left(\hat{b} + \hat{b}^{\dagger}\right)$ are dimensionless momentum and position operators for BEC with commutation relation, $[\hat{Q}, \hat{P}] = i$ and $\Omega = 4\omega_r = 2\hbar k^2/m_a$, is recoil frequency of an atom. Third term in eq. (5) describes coupled energy of field and condensate with coupling strength $\xi_{sm} = (\omega_c)/(L)(\hbar/m_{bec}4\omega_r)^{1/2}$, where, $m_{bec} = \hbar\omega_c^2/(L^2 N U_0^2 \omega_r)$ is the side mode mass of condensate. The last term accounts for the coupling of BEC with transverse field and $\eta_{eff} = (n)^{1/2}\eta_{\perp}$ is transverse coupling strength.

The Hamiltonian for the part of moving-end mirror $\hat{H}_{MF}$ can be given as[45],

$$\hat{H}_{MF} = \hbar\Delta_c\hat{c}^{\dagger}\hat{c} + \frac{\hbar\omega_m}{2}(\hat{p}^2 + \hat{q}^2) - \xi\hbar\hat{c}^{\dagger}\hat{c}\hat{q} - i\hbar\eta(\hat{c} - \hat{c}^{\dagger}), \tag{6}$$

first term is associated with energies of the intra-cavity field where, $\Delta_c = \omega_c - \omega_p$ is external pump field and intra-cavity field detuning, ω_c is intra-cavity field frequency and $\hat{c}^{\dagger}$ ($\hat{c}$) are creation (annihilation) operators for intra-cavity field with commutation relation $[\hat{c}, \hat{c}^{\dagger}] = 1$. Second term describes the motion of moving-end mirror where, $\hat{q}$ and $\hat{p}$ are dimensionless position and momentum operators for moving-end mirror respectively, having commutation relation $[\hat{q}, \hat{p}] = i$, which reveals the value of the scaled Planck's constant, $\hbar = 1$. Third term represents coupling of moving-end mirror with field generated by radiation pressure applied by intra-cavity field on moving-end mirror. Here $\xi = (2)^{1/2}(\omega_c/L)x_0$ is the coupling strength and $x_0 = (\hbar/2m\omega_m)^{1/2}$, is zero point motion of mechanical mirror having mass m. Last term is associated with the coupling of intra-cavity field with external pump field $|\eta| = (P\kappa/\hbar\omega_p)^{1/2}$, where, κ is cavity decay rate related with outgoing modes and P is the external pump field power.

The Hamiltonian $\hat{H}_T$ describes the effects of dissipation and noises associated with optomechanical system by using standard quantum noise operators[46]. The total Hamiltonian H leads to develop coupled quantum Langevin equations for optical, mechanical (moving-end mirror) and atomic (BEC) degrees of freedom.

$$\frac{d\hat{c}}{dt} = \dot{\hat{c}} = (i\widetilde{\Delta} + i\xi\hat{q} - i\xi_{sm}\hat{Q} - \kappa)\hat{c} + i\eta_{eff}\hat{Q} + \eta + \sqrt{2\kappa a_{in}}, \tag{7}$$

$$\frac{d\hat{p}}{dt} = \dot{\hat{p}} = -\omega_m\hat{q} - \xi\hat{c}^{\dagger}\hat{c} - \gamma_m\hat{p} + \hat{f}_B, \tag{8}$$

$$\frac{d\hat{q}}{dt} = \dot{\hat{q}} = \omega_m\hat{p}, \tag{9}$$

$$\frac{d\hat{P}}{dt} = \dot{\hat{P}} = -4\omega_r\hat{Q} - \xi_{sm}\hat{c}^{\dagger}\hat{c} - \gamma_a\hat{P} + \hat{f}_{1m}, \tag{10}$$

$$\frac{d\hat{Q}}{dt} = \dot{\hat{Q}} = 4\omega_r\hat{P} - \gamma_a\hat{Q} + \hat{f}_{2m}. \tag{11}$$

$\widetilde{\Delta} = \Delta_c - NU_0/2$ is the effective detuning of the system and $\hat{a}_{\text{in}}$ is Markovian input noise associated with intra-cavity field. The term γ_m describes mechanical energy decay rate of the moving-end mirror and $\hat{f}_B$ is Brownian noise operator associated with the motion of moving-end mirror[47,48]. The term γ_a represents damping of BEC due to harmonic trapping potential which affects momentum side modes while, $\hat{f}_{1M}$ and $\hat{f}_{2M}$ are the associated noise operators assumed to be Markovian.

As we focused on the the bistable behavior of optomechanics and its classical dynamics, we consider positions and momenta as classical variables. To write the steady- state values of the operator we assume optical field decay at its fastest rate so that, we can set time derivative to zero in equation (7). The steady-state values of operators are given as,

$$c_s = \frac{\eta + i\eta_{eff}Q}{\kappa + i(\Delta_a - \xi q + \xi_{sm}Q)}, \tag{12}$$

$$q_s = \frac{\xi c^{\dagger}c}{\omega_m}, \tag{13}$$

$$p_s = 0, \tag{14}$$

$$Q_s = \frac{-\xi_{sm}c^{\dagger}c}{4\omega_r[1 - \gamma_a/4\omega_r]}, \tag{15}$$

$$P_s = \frac{\gamma_a}{4\omega_r}Q_s. \tag{16}$$

The steady-state photons number of intra-cavity field is described as,

$$n_s = |c_s|^2 = \frac{\eta^2 + \eta_{eff}^2Q^2}{\kappa^2 + (\Delta_a - \xi q + \xi_{sm}Q)^2}. \tag{17}$$

Optical, BEC and moving-end mirror Bistability

The hybrid BEC-optomechanical system shown in Fig. 1 is simultaneously driven by external pump field with frequency ω_p. When intra-cavity radiation pressure oscillates with frequency (ω_c) is equal to the frequency of moving-end mirror ω_m, it generates the Stokes and anti-Stokes scatterings of light from the intra-cavity field potential. Conventionally, optomechanical systems are operated in resolved-sideband regime $\kappa << \omega_m$, which is off-resonant with Stokes scattering, therefore, the Stokes scattering is strongly suppressed and only anti-Stokes scattering will survive inside the cavity potential which causes the

conversion of external pump photons to the intra-cavity photons. Therefore, by increasing the external pump field strength, the anti-Stokes scattering of intra-cavity photon number will be increased and will cause to move system in bistable regime. Optical bistability has been discussed in optomechanics in Ref 36. by considering double cavity configuration and the effects of s-wave scattering on bistable behavior of intra-cavity photon number have been studied in Ref. 49. In our optomechanical configuration, we consider transverse optical field to control the bistable behavior of the system. The idea is motivated by the findings of Ref. 39, where, they use transverse optical field to control bistable behavior of intra-cavity photons induced by external pump field. This mechanism provides another source of inducing photons in the cavity-optomechanics. It can be easily noticed from mathematical description that how this perpendicular channel of photon influence the optomechanical system and how it is connected to the displacement of atomic mode of the system. Therefore, the transverse photons will scatter inside the cavity depending on the configuration of intra-cavity condensate mode and will behave as nonlinear factor to the intra-cavity photon number.

To obtain the steady-state relation for Intra-cavity photon number, we use expression (17) and substitute the steady state values of position corresponding to moving-end mirror and condensate.

$$n_s = \frac{\eta^2 + \eta_{eff}^2 \left(\frac{-\xi_{sm} n_s}{4\omega_r [1 - \gamma_a / 4\omega_r]} \right)^2}{\kappa^2 + \left(\Delta_a - \xi \left(\frac{\xi n_s}{\omega_m} \right) + \xi_{sm} \left(\frac{-\xi_{sm} n_s}{4\omega_r [1 - \gamma_a / 4\omega_r]} \right) \right)^2}. \tag{18}$$

Figure 2 shows the bistable behavior of intra-cavity photon number under the influence of transverse optical field. We obtain optical bistability results by solving equ.(18). In Fig. 2(a), the blue curve represents intra-cavity photon number as function of external pump field strength (η/κ) when the transverse field strength is zero ($\eta_{eff}/\kappa = 0$). We can observe, third order roots exist for photon number corresponding to single value of external pump field, which cause the appearance of bistability in intra-cavity photon number[39]. In Fig. 2(a), red curve shows optical bistability when the value of transverse optical field intensity is $\eta_{eff}/\kappa = 200$ and green curve shows optical bistability when transverse optical field intensity is $\eta_{eff}/\kappa = 400$. By observing the red and the green curves in Fig. 2(a), one can easily note that the strength of optical bistability is changed by changing the intensity of transverse optical field. The transverse optical field directly interacts with the intra-cavity atomic mode or BEC, trapped inside optomechanical system and is the reason for scattering of photons inside the cavity. Therefore, optical bistability curve is modified by increasing the strength of perpendicular nonlinearities. In short, photon bistability of intra-cavity potential is tunable with the help of perpendicular field. 2(b) shows the continuous behavior of intra-cavity photon bistability as a function of external pump field and transverse optical field, which provides better understanding of the control of intra-cavity optical mode with transverse optical field strength.

Further, to understand the influence of transverse field on intra-cavity optical mode, we study the optical behavior of the system with different values of effective detuning. Fig. 2(c) shows the intra-cavity optical bistability as a function of external pump field and effective detuning of the system in the absence of transverse field. We observe the tilted behavior of photonic peaks which represents bistable behavior of photon number. Fig. 2(d) and Fig. 2(e) represent similar behavior for different values of transverse field intensity $\eta_{eff}/\kappa = 40,50$, respectively. These findings more efficiently clarify the intra-cavity optical mode dependence on perpendicularly interacting photons. Initially, intra-cavity optical mode exits only when it is resonant with external pump field. But when we increase the strength of external pump field, a tilt appear in the optical mode due to the influence of atomic mode and by increasing the value of transverse field, the strength of optical mode show enhancement and it is more tilted towards negative detuning of the system. By following these results, we can confidently state that the bistability of optical mode is tunable with the help of transverse optical field.

Transverse optical field cause the the scattering of photons inside the cavity and this scattering can be controlled by the strength of transverse optical field. If we increase the strength of transverse field to large values, scattered photons inside the cavity will fill the upper branch of bistability and will cause the suppression of optical bistability (see Ref. 39). Figure 3(a) demonstrates such behavior of intra-cavity photon at higher value of transverse field. Blue, yellow, red and green curve corresponds to the bistable behavior of intra-cavity photon number at transverse field strengths $\eta_{eff}/\kappa = 400$, 800, 2000, 3000, respectively. We can note that by increasing strength of perpendicular field, intra-cavity photons start saturating in upper branch of bistability caused by external driving field and the population of photons in upper branch becomes much larger than the photons in lower branch of bistablity which leads to the suppression of lower stable state. Fig.(b) shows the behavior of upper stable state of bistability with large transverse field strengths. Similarly, blue, yellow, red and green curve contain information about the behavior of upper stable state at transverse field strengths $\eta_{eff}/\kappa = 3000$, 3500, 4000, 4500, respectively and show continuous enhancement in the upper branch population with increase in transverse optical field.

To study the bistable dynamics of atomic mode or condensate mode of the system and mechanical mode or moving-end mirror of cavity-optomechanics, we rewrite the steady-state solution for position of both modes as,

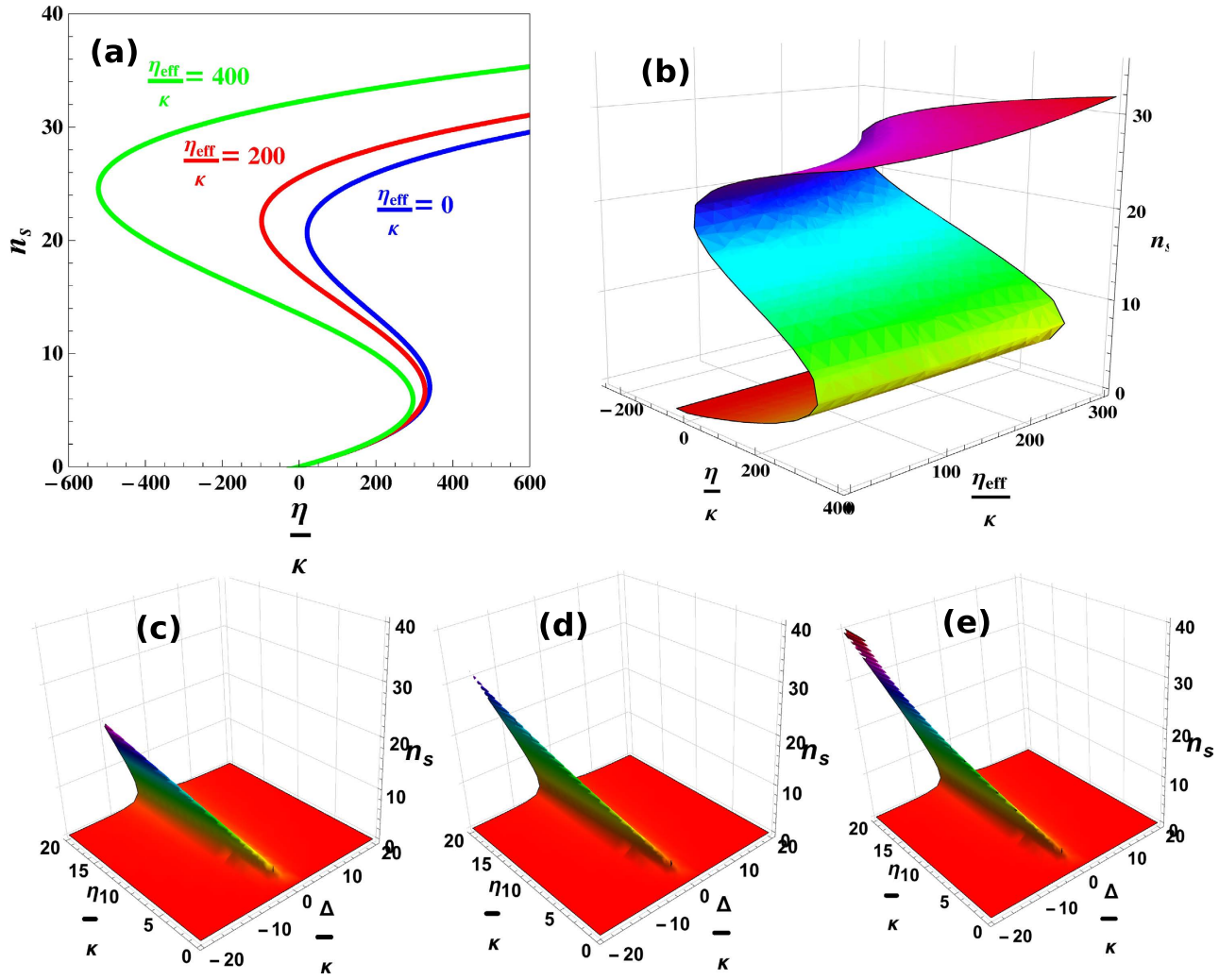

Figure 2. Tunable optical bistability of intra-cavity field. (**a**) shows optical bistability as a function of external pump field (η/κ) for different values of transverse optical field. Blue, red and green curves are for transverse optical field strength $\eta_{eff}/\kappa = 0,200,400$, respectively. (**b**) shows the continuous behavior of intra-cavity photon number as a function of interacting transverse field strength (η_{eff}/κ) and external pump field strength (η/κ). (**c**) represents optical behavior of intra-cavity field as a function of external field strength (η/κ) and effective detuning (Δ/κ) of the system in the absence of transverse optical field intensity ($\eta_{eff}/\kappa = 0$). Similarly, (**d**) and (**e**) show optical bistability as a function of external field (η/κ) and effective detuning (Δ/κ) for transverse field strength $\eta_{eff}/\kappa = 25,42$, respectively. All numerical parameters are considered from given experimental parameters.

$$q_s = \frac{\xi\left(\eta^2 + \eta_{eff}^2 Q^2\right)}{\omega_m(\kappa^2 + (\Delta_a - \xi q + \xi_{sm} Q)^2)}, \tag{19}$$

$$Q_s = \frac{-\xi_{sm}\left(\frac{\eta^2 + \eta_{eff}^2 Q^2}{\kappa^2 + (\Delta_a - \xi q + \xi_{sm} Q)^2}\right)}{4\omega_r[1 - \gamma_a/4\omega_r]}. \tag{20}$$

To discuss bistability effects on the intra-cavity potential, we derive couple equation of motion for both, moving end mirror and BEC by treating their motion of moving-end mirror and BEC classically and assuming time scale very short so that their mechanical damping can be ignored. We write the couple equations of motion by using the quantum Langevin equations as,

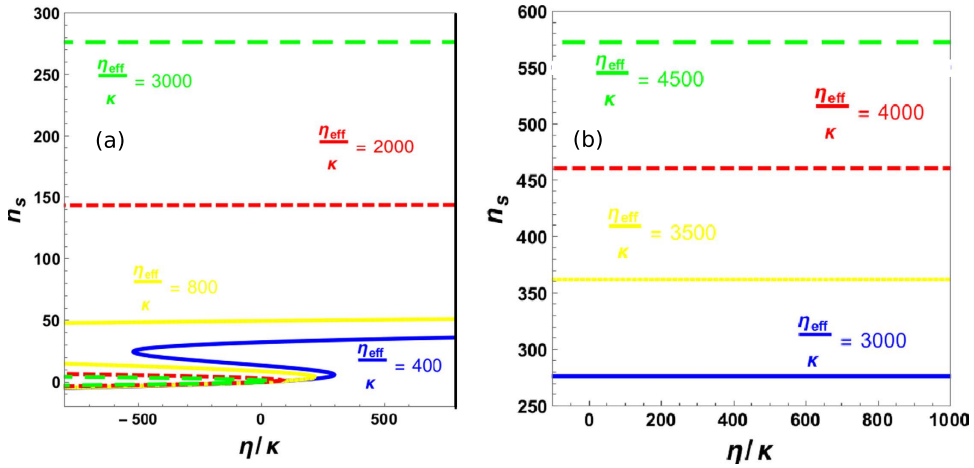

Figure 3. Suppression of Bistability with transverse field. Suppression of intra-cavity optical mode bistability with large values of transverse optical field. In (**a**), blue, yellow, red and green curve corresponds to the bistable behavior of intra-cavity photon number at transverse field strengths $\eta_{eff}/\kappa = 400$, 800, 2000, 3000, respectively. (**b**) accommodates the response of upper stable state of bistability at higher values of transverse optical field. Similarly, blue, yellow, red and green curve represent upper branch photon number at transverse field strengths $\eta_{eff}/\kappa = 3000$, 3500, 4000, 4500, respectively. All numerical parameters are used from given experimental parameters.

$$\frac{d^2q}{dt^2} = -\omega_m^2 q + \frac{\omega_m \xi \left(\eta^2 + \eta_{eff}^2 Q^2\right)}{\kappa^2 + (\Delta + \xi q - \xi_{sm} Q)^2}, \tag{21}$$

$$\frac{d^2Q}{dt^2} = -(4\omega_r)^2 Q - \frac{4\omega_r \xi_{sm}\left(\eta^2 + \eta_{eff}^2 Q^2\right)}{\kappa^2 + (\Delta + \xi q - \xi_{sm} Q)^2}. \tag{22}$$

By using these coupled equation, we derive the effective potential of the intra-cavity field,

$$V = -\frac{\omega_m^2 q^2}{2} - \frac{(4\omega_r)^2 Q^2}{2} + \int \frac{\omega_m \xi \left(\eta^2 + \eta_{eff}^2 Q^2\right)}{\kappa^2 + (\Delta + \xi q - \xi_{sm} Q)^2} dq - \int \frac{4\omega_r \xi_{sm}\left(\eta^2 + \eta_{eff}^2 Q^2\right)}{\kappa^2 + (\Delta + \xi q - \xi_{sm} Q)^2} dQ. \tag{23}$$

It is known that mechanical degree of freedom (moving-end mirror) and atomic degree of freedom (condensate) are coupled with each other through intra-cavity optical mode. The modulation in intra-cavity photon number modify the quantity of radiation pressure exerted on atomic and mechanical mode of the system. We have already discussed the bistable behavior of intra-cavity field. Now we illustrate that the steady-state position of both atomic mode (Q_s) as well as moving-end mirror (q_s) possess same properties of bistability as optical mode of the system by using equation (19) and (20).

Figure 4 demonstrates the bistable dynamics of moving-end mirror of optomechanical system and Cigar-Shaped Bose-Einstein condensate (BEC) trapped inside optomechanical system in the presence of transverse optical field. Fig. 4(a) and Fig. 4(b) show bistable behavior of moving-end mirror position q and BEC position Q as a function of external field strength in the absence of transverse optical field ($\eta_{eff}/\kappa = 0$). As equation (19) and (20) are third-ordered equations for both moving-end mirror and BEC, respectively, so by solving these equations, we obtain three roots which lead us to the occurrence of bistable behavior. Fig. 4(c) shows the effective potential V as a function of mechanical mode and atomic mode steady-state position. These results are obtained by solving expression for effective potential (24) and steady-state values for the position of moving-end mirror and BEC. The potential V, shown in Fig. 4(c), is generally illustrated as two-dimensional double-well potential. The two local minima A and B corresponding to the stable points $\{q_A, Q_A\}$ and $\{q_B, Q_B\}$ are shown in Fig. 4(a) and Fig. 4(b). These two points represent two stable regions in effective potential of the optomechanical system in accordance to the particular set of values of moving-end mirror position and BEC position. The point C in effective potential V, shown in Fig. 4(c) is a saddle-point corresponding to values $\{q_c, Q_c\}$ in Fig. 4(a) and Fig. 4(b). Saddle-point represents unstable behavior of the effective potential of system which means at certain particular values of moving-end mirror position and BEC position, system possesses chaotic behavior, as illustrated in many classical systems such as[50,51].

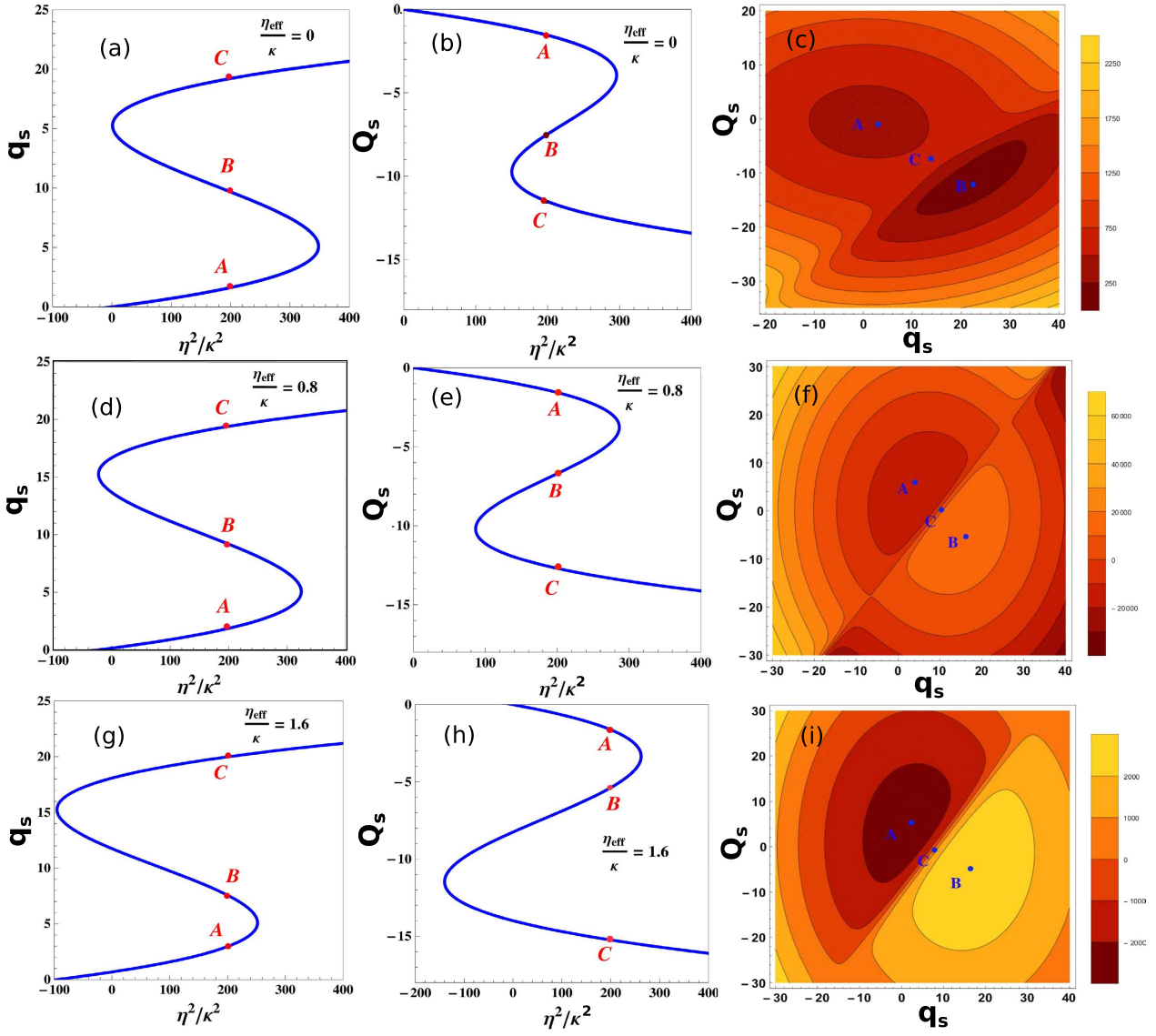

Figure 4. The bistable dynamics of Bose-Einstein condensate and moving-end mirror of cavity. The bistable behavior of moving-end mirror position q and Cigar-shaped BEC position Q for the different values of transverse field intensities. (**a**) and (**b**) show bistability of moving-end mirror position and BEC position, respectively, as a function of external pump field and in the absence of transverse optical field ($\eta_{eff}/\kappa = 0$). (**c**) demonstrates the effective potential of the optomechanical system as a function of moving-end mirror position and BEC position. Points A, B and C in (**c**) correspond to the points $\{q_A,Q_A\}$, $\{q_B,Q_B\}$ and $\{q_C,Q_C\}$, respectively, as shown in (**a**) and (**b**). Similarly, (**d**) and (**e**) represent bistability of moving-end mirror and BEC, respectively, at the value of transverse optical field $\eta_{eff}/\kappa = 0.8$ and (**f**) shows their effects on the effective potential of the system. (**g**) and (**h**) represent bistability of moving-end mirror and BEC at transverse optical field strength $\eta_{eff}/\kappa = 1.6$ and (**i**) shows their effects on the effective potential of the system. Similarly, the points A, B and C, in (**f**) and (**i**), correspond to the points given in bistable BEC and moving-end mirror positions results. All numerical parameters are driven by given experimental parameters.

Figure 4(d) and Fig. 4(e) show bistable behavior of moving-end mirror position q and BEC position Q as a function of external pump field with transverse optical field strength $\eta_{eff}/\kappa = 0.8$ and Fig. 4(f) shows their collective influence on the behavior of effective potential of optomechanical system. We observe the similar behavior, as we discuss earlier in Fig. 4(c), but due to the presence of transverse optical field, the stable and unstable regions are now modified and the values of stable points and saddle-point are changed. The photons interacting perpendicularly with system through transverse field are directly associated with intra-cavity atomic momentum side modes which are bounded with mechanical mode (moving-end mirror) in relation of radiation pressure. Therefore, a minute variation in the strengths of transverse field cause modified bistable behavior of intra-cavity atomic mode Q_s and mechanical mode

q_s. Moreover, the perpendicularly scattering photons inside the cavity drive momentum side modes of BEC and apply radiation pressure on mirror even when there is no external pump field. According to equation (24), effective potential of system completely relies on position of moving-end mirror and BEC. Therefore, a small change in bistable behavior of their positions can bring notable modification in effective potential of the system, as shown in Fig. 4(f), which means the stable points *A* and *B*, shown in Fig. 4(f), are not the same as in Fig. 4(c) and saddle-point *C* is also different from the saddle-point in Fig. 4(c) because of the variations in the bistability of moving-end mirror position and BEC position. Figure 4(g) and Fig. 4(h) illustrate the similar behavior of bistability of moving-end mirror position and BEC position at different transverse optical field strength $\eta_{eff}/\kappa = 1.6$ and Fig. 4(i) shows their mutual effects on the effective potential. These results also assert the effectiveness of previous one that the values of both stable points as well as saddle-point are changed due to the increase in transverse field strength which cause modification in stable and unstable regions in effective potential. By observing these results, one can conclude that the bistable dynamics of moving-end mirror as well as BEC are tunable with the help of transverse optical field.

It is very important to observe time dependent dynamics of atomic mode and mechanical mode of the system. In this section, we will discuss the temporal behavior of Q and q and see how transverse optical field will influence their temporal dynamics. Figure 5 accounts for the time dependent response of moving-end mirror and Bose-Einstein condensate corresponding to different transverse optical field strengths, in quasi-periodic regime as shown in Fig. 4, initially located at $\{q = 0, Q = 0\}$. We solve quantum langevin equation to obtain the spatial dynamics of intra-cavity atomic mode and mechanical mode of the system under the assumption that the position operator for BEC (Q) and moving-end mirror (q) behaves like classical variables which allow us to ignore quantum noise effects associated with the optomechanical system. Figure 5(a) represents behavior of moving-end mirror with respect to time $\omega_m t$ corresponding to different transverse field strengths. Green line shows the behavior of moving-end mirror in the absence of transverse optical field ($\eta_{eff}/\kappa = 0$). The moving-end mirror follows continuous oscillatory behavior with particular amplitudes corresponding with time as discussed in[15]. The red line represents time dynamics of moving-end mirror when transverse field strength is $\eta_{eff}/\kappa = 0.8$. We can clearly detect that the amplitudes of oscillations of moving-end mirror have been increased by increasing transverse optical field, which cause a shift in moving-end mirror position from stable regime to unstable regime (chaotic regime), as shown in Fig. 4(f). Similarly, blue curve demonstrates time dependent dynamics of moving-end mirror for $\eta_{eff}/\kappa = 1.8$ and shows that the oscillatory behavior of moving-end mirror is different from the other curves because of the increase in transverse field. Transverse optical field directly modulates the intra-cavity field potential which effectively brings nonlinearities to the system and therefore, cause chaotic behavior of moving-end mirror.

Figure 5(b) illustrates time dependent behavior of intra-cavity atomic mode (BEC) under the influence of transverse field strength. Green curve is associated with time dependent response of BEC in the absence of transverse field ($\eta_{eff}/\kappa = 0$). We can note that atomic mode possesses similar temporal oscillatory behavior with particular amplitudes like moving-end mirror. The red line represents time dynamics of BEC at perpendicular optical field ($\eta_{eff}/\kappa = 0.8$). We observe that the amplitude of oscillations of intra-cavity atomic mode is attenuated because transverse field photons are associated with the position of BEC and cause the suppression of time dependent oscillations of atomic momentum side modes. Similarly, blue curve represents the effects of transverse field ($\eta_{eff}/\kappa = 1.8$) on the spatial dynamics of BEC. Demonstration of these results enable us to conclude that the time dependent dynamics of BEC and moving-end mirror of optomechanics are also controllable using transverse field.

In order to observe the behavior of effective potential V with respect to the intra-cavity photon number, we derive the expression of effective potential (equ. (24)) by considering the steady-state values for the position of moving-end mirror and BEC (equ. (13) and (15)) as,

$$V_s = -\frac{\omega_m(\xi n_s)^2}{2} + \frac{4\omega_r(\xi_{sm} n_s)^2}{2[1-\gamma_a/4\omega_r]^2} + \int \frac{\xi^2(\eta^2 - \eta_{eff}^2\left(\frac{\xi_{sm} n_s}{4\omega_r[1-\gamma_a/4\omega_r]}\right)^2)}{\kappa^2 + \left(\Delta + \xi\left(\frac{\xi n_s}{\omega_m}\right) + \xi_{sm}\left(\frac{\xi_{sm} n_s}{4\omega_r[1-\gamma_a/4\omega_r]}\right)\right)^2} dn_s + \int \frac{\frac{\xi_{sm}^2}{[1-\gamma_a/4\omega_r]}(\eta^2 - \eta_{eff}^2\left(\frac{\xi_{sm} n_s}{4\omega_r[1-\gamma_a/4\omega_r]}\right)^2)}{\kappa^2 + \left(\Delta + \xi\left(\frac{\xi n_s}{\omega_m}\right) - \xi_{sm}\left(\frac{\xi_{sm} n_s}{4\omega_r[1-\gamma_a/4\omega_r]}\right)\right)^2} dn_s. \quad (24)$$

Figure 6 demonstrates the relation of effective potential of cavity-optomechanics with the intra-cavity photon number and parallel driving field under the influence of transverse optical field. Fig. 6(a) shows that effective potential of the system increases monotonically with increase in external pump field and intra-cavity photon number in the absence of transverse optical field. Fig. 6(b) represents the similar behavior effective potential but in the presence of transverse pump field strength $\eta_{eff}/\kappa = 0.8$. Effective

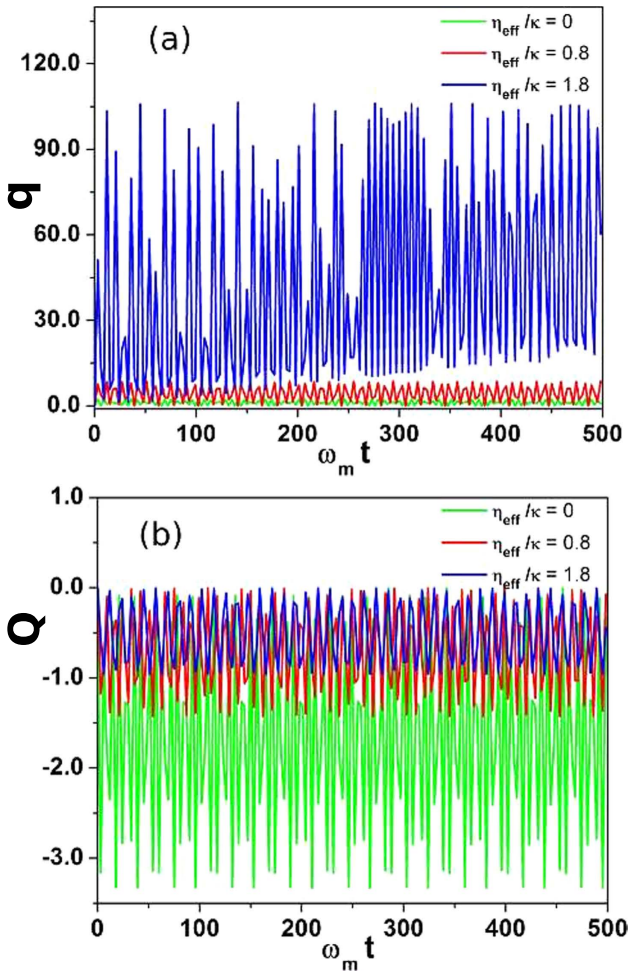

Figure 5. Temporal behavior of Bose-Einstein condensate and moving-end mirror. The temporal behavior of Bose-Einstein condensate position Q and moving-end mirror q as a function of transverse optical field strength η_{eff}/κ. (**a**) describes the time dependent behavior of moving-end mirror position for different transverse field strengths. Green line shows moving-end mirror position as a function of time ($\omega_m t$) in the absence of transverse optical field ($\eta_{eff}/\kappa = 0$). The red line represents temporal response of moving-end mirror when transverse field strength is $\eta_{eff}/\kappa = 0.8$ and blue line accommodates time dependence of moving-end mirror at transverse field $\eta_{eff}/\kappa = 1.8$. (b) demonstrates time dependent dynamics of Bose-Einstein condensate position corresponding to different transverse field strengths. Green curve corresponds to the temporal response of BEC in the absence of transverse field ($\eta_{eff}/\kappa = 0$). Red and blue lines represent time dependent behavior of BEC corresponding to $\eta_{eff}/\kappa = 0.8$ and $\eta_{eff}/\kappa = 1.8$, respectively. The strength of external driving field is $\eta = 18.4 \times 2\pi MHz$ and optical detuning of the system is considered as $\Delta = 0.52 \times 2\pi MHz$. The remaining numerical parameters are same as in previous results.

potential shows monotonic behavior with increase in parallel field but because of the presence of transverse field another curvature appears in effective potential. When perpendicular optical field interacts with intra-cavity atomic mode, it causes the scattering of photons inside the cavity depending upon the configuration of atomic mode which lead to the modification in intra-cavity effective optical potential. We can note the existence of photons inside the cavity in the absence of external pump field because of the transverse field scattering from condensates. This scattering also causes the existence of homogeneous atomic side modes. 6(b) clearly shows such modulation in the effective potential of the system.

Figure 6(c) represents the response of effective potential inside the cavity at different transverse optical field strength $\eta_{eff}/\kappa = 1.2$. We observe that the curvature appeared in effective potential with intra-cavity photon number is enhanced due to the increase in transverse photon scattering. Figure 6(d–f) illustrate similar behavior of effective intra-cavity potential and photon number with transverse optical field strength $\eta_{eff}/\kappa = 1.6$, $\eta_{eff}/\kappa = 2$ and $\eta_{eff}/\kappa = 2.4$, respectively and show continuous enhancement in nonlinear curvature appearing in effective potential of the system with transverse photon interaction. These findings lead us to control the collective behavior of intra-cavity optical potential with the help of transverse optical field and enable us to understand the explicit nature of hybrid optomechanical systems.

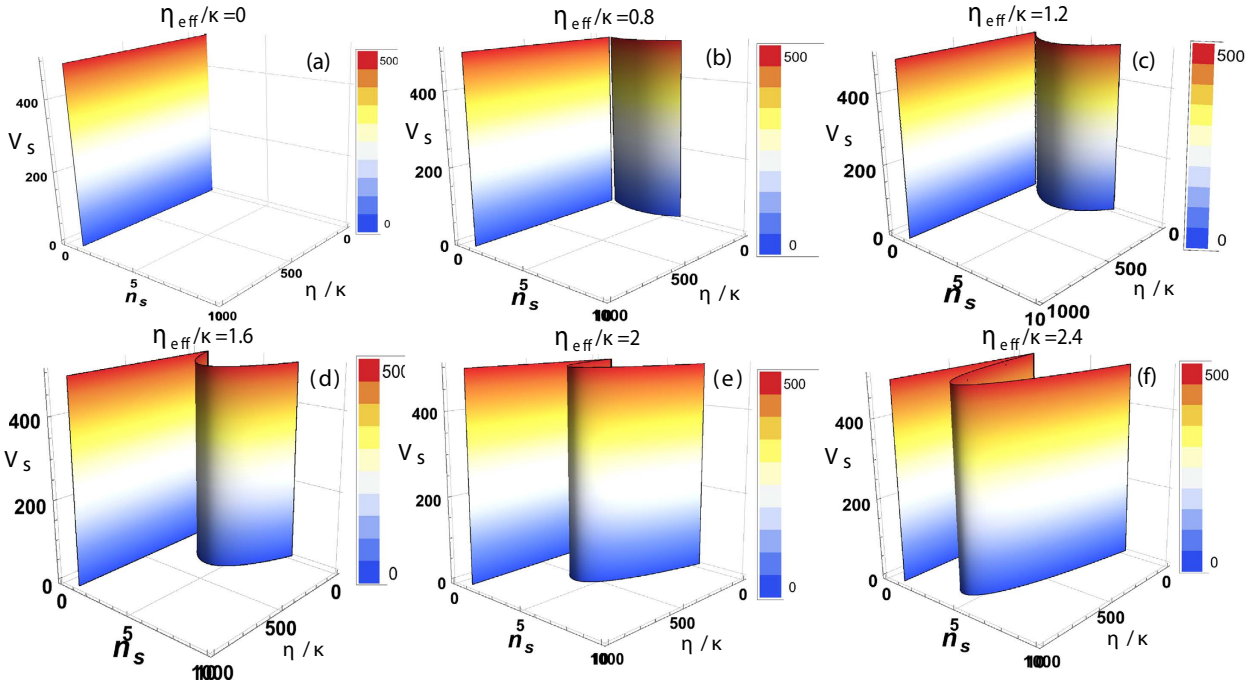

Figure 6. Transverse field effect on effective potential. The continuous behavior of effective potential of optomechanical system as a function of intra-cavity photon number and external pump field strength with different transverse field strengths. (**a**) demonstrates the behavior of intra-cavity effective potential with respect to photon number and external driving field coupling η/κ in the absence of transverse field η_{eff}/κ. (**b**) shows the effective potential when the transverse field strength is $\eta_{eff}/\kappa = 0.8$. (**c**) represents the effects of transverse field strength $\eta_{eff}/\kappa = 1.2$ on the effective potential. Similarly, (**d**) shows effective potential for transverse field $\eta_{eff}/\kappa = 1.6$. (**e**) and (**f**) demonstrate the effective potential of the system for transverse optical field $\eta_{eff}/\kappa = 2$ and $\eta_{eff}/\kappa = 2.4$, respectively. The remaining parameters are same as in above discussion.

Discussion and Conclusion

In this report, we discuss the bistable dynamics of hybrid BEC-optomechanics. We consider $N = 2.3 \times 4$ ^{87}Rb atoms trapped inside Fabry-Pérot cavity with length $L = 1.25 \times 10^{-4}$, with a moving-end mirror and driven by single mode external field with power $P_{in} = 0.0164mW$, frequency $\omega_p = 3.8 \times 2\pi \times 10^{14}\,Hz$ and wavelength $\lambda_p = 780nm$. The moving-end mirror of cavity should be a perfect reflector and performs oscillations, because of intra-cavity field radiation pressure, with frequency $\omega_m = 15.2 \times 2\pi MHz$ and its coupling with intra-cavity field is considered as $\xi = 3.8\,MHz$. The frequency of intra-cavity field is $\omega_c = 15.3 \times 2\pi \times 10^{14}\,Hz$, with cavity decay rate $\kappa = 1.3 \times 2\pi kHz$. Intra-cavity field produces recoil of $\omega_r = 3.8 \times 2\pi kHz$ in atoms trapped inside cavity. The coupling of intra-cavity field with BEC is $\xi_{sm} = 4.4\,MHz$. Detuning of the system is taken as $\Delta = \Delta_c + (U_0 N)/(2) = 0.52 \times 2\pi MHz$, where vacuum Rabi frequency of the system is $U_0 = 3.1 \times 2\pi MHz$. We use a transverse optical field, with frequency $\omega_\perp$ and coupling $\eta_\perp$, to control the bistable dynamics of hybrid system. Our results demonstrate that the optical bistability of the system is controllable by using transverse optical field because the perpendicularly interacting photons are coupled to atomic momentum side modes, exited by the motion of Bose-Einstein condensate due to the interaction of intra-cavity field. We have also discussed the spatial bistability of moving-end mirror and BEC with different values of transverse field strength and thus, have shown that the bistable dynamics of moving-end mirror and BEC are tunable using transverse optical field intensity and studied their effects on effective potential. We further illustrated the temporal behavior of mechanical mode and atomic mode (BEC) of the system and found that the dynamics of mechanical mode can be pushed to chaotic regime by increasing the strength of vertical field. Besides, we studied the variance in effective potential of the system as a function of cavity photon number and external driving field under the influence of transverse field and found out magnificent nonlinear response of effective potential with perpendicularly scattering photons. This method provides us an excellent control over the nonlinear dynamics of such hybrid systems.

In future, we will explore the nonlinear dynamics of hybrid system in good cavity limits and will also study the controllable dynamics by considering interacting Bose-Einstein condensate. Besides, we intend to extend this method to examine the controllability of novel phenomenon like electromagnetically induced transparency and entanglement. Additional goals include the discussion on the effects of spin-orbit coupling using magnetic field in hybrid BEC-optomechanical systems.

References

1. Kippenberg, T. J. & Vahala, K. J. Cavity Optomechanics: Back-Action at the Mesoscale, *Science* **321,** 1172 (2008).
2. Brennecke, F., Ritter, S., Donner, T. & Esslinger, T. Cavity optomechanics with a Bose-Einstein condensate, *Science* **322,** 235 (2008).
3. OConnell, A. D. *et al.* Quantum ground state and single-phonon control of a mechanical resonator, *Nature* **464,** 697 (2010).
4. Teufel, J. D. *et al.* Sideband cooling of micromechanical motion to the quantum ground state, *Nature* **475,** 359 (2011).
5. Chan, J. *et al.* Laser cooling of a nanomechanical oscillator into its quantum ground state, *Nature* **478,** 89 (2011).
6. Liu, K., Tan, L., Lv, C. H. & Liu, W. M. Quantum phase transition in an array of coupled dissipative cavities, *Phys. Rev. A* **83,** 063840 (2011).
7. Sun, Q., Hu, X. H., Ji, A. C. & Liu, W. M. Dynamics of a degenerate Fermi gas in a one-dimensional optical lattice coupled to a cavity, *Phys. Rev. A* **83,** 043606 (2011).
8. Teufel, J. D. *et al.* Circuit cavity electromechanics in the strong-coupling regime, *Nature* **471,** 204 (2011).
9. Groeblacher, S., Hammerer, K., Vanner, M. R. & Aspelmeyer, M. Observation of strong coupling between a micromechanical resonator and an optical cavity field, *Nature* **460,** 724 (2009).
10. Teufel, J. D. *et al.* Quantum mechanics: A light sounding drum, *Nature* **471,** 204 (2011).
11. Verhagen, E., Deleglise, S., Weis, S., Schliesser, A. and Kippenberg, T. J. Quantum-coherent coupling of a mechanical oscillator to an optical cavity mode, *Nature* **482,** 63 (2012).
12. Braginsky, V. & Vyatchanin, S. P. Low quantum noise tranquilizer for FabryPerot interferometer, *Phys. Lett. A* **293,** 228 (2002).
13. Rugar, D. *et al.* Single spin detection by magnetic resonance force microscopy, *Nature* **430,** 329 (2004).
14. Echenfield, M. *et al.* Optomechanical crystals, *Nature* **462,** 78 (2009).
15. Zhang, K., Chen, W., Bhattacharya, M. & Meystre, P. Hamiltonian chaos in a coupled BECoptomechanical-cavity system, *Phys. Rev. A* **81,** 013802 (2010).
16. Ying-Dan Wang & Clerk, A. A. Using Interference for High Fidelity Quantum State Transfer in Optomechanics, *Phys. Rev. Lett.* **108,** 153603 (2012).
17. Singh, S. *et al.* Quantum-state transfer between a Bose-Einstein condensate and an optomechanical mirror, *Phys. Rev. A* **86,** 021801 (2012).
18. Abdi, M. *et al.* Continuous-variable-entanglement swapping and its local certification: Entangling distant mechanical modes, *Phys. Rev. A* **89,** 022331 (2014).
19. Abdi, M. *et al.* Entanglement Swapping with Local Certification: Application to Remote Micromechanical Resonators, *Phys. Rev. Lett.* **109,** 143601 (2012).
20. Sete, E. A. *et al.* Light-to-matter entanglement transfer in optomechanics, *J. Opt. Soc. Am. B* **31,** 2821 (2014).
21. Hofer, S. G. *et al.* Quantum entanglement and teleportation in pulsed cavity-optomechanics, *Phys. Rev. A* **84,** 052327 (2011).
22. Buchmann, L. F. *et al.* Macroscopic Tunneling of a Membrane in an Optomechanical Double-Well Potential, *Phys. Rev. Lett.* **108,** 210403 (2012).
23. Agarwal, G. S. & Huang, S. Electromagnetically induced transparency in mechanical effects of light, *Phys. Rev. A* **81,** 041803(R) (2010).
24. Weis, S. *et al.* Optomechanically Induced Transparency, *Science* **330,** 1520 (2010).
25. Peng, B. *et al.* What is and what is not electromagnetically induced transparency in whispering-gallery microcavities, *Nat. Commun.* **10,** 1038 (2014).
26. Safavi-Naeini, A. H. *et al.* Electromagnetically induced transparency and slow light with optomechanics, *Nature* **472,** 69 (2011).
27. Yasir, K. A., Ayub, M. & Saif, F. Exponential localization of moving-end mirror in optomechanical system, *J. Mod. Opt.* **61,** 1318 (2014).
28. Ayub, M., Yasir, K. A. & Saif, F. Dynamical localization of matter waves in optomechanics, *Laser Phys.* **24,** 115503 (2014).
29. Jin, G. R. & Liu, W. M. Collapses and revivals of exciton emission in a semiconductor microcavity: Detuning and phase-space filling effects, *Phys. Rev. A* **70,** 013803 (2004).
30. Ji, A. C., Xie, X. C. & Liu, W. M. Quantum magnetic dynamics of polarized light in arrays of microcavities, *Phys. Rev. Lett.* **99,** 183602 (2007).
31. Ji, A. C., Sun, Q., Xie, X. C. & Liu, W. M. Josephson effect for photons in two weakly linked microcavities, *Phys. Rev. Lett.* **102,** 023602 (2009).
32. Tan, L., Zhang, Y. Q. & Liu, W. M. Quantum phase transitions for two coupled cavities with dipole-interaction atoms, *Phys. Rev. A* **84,** 063816 (2011).
33. Yi-Xiang, Y. Ye, J. & Liu, W. M. Goldstone and Higgs modes of photons inside a cavity, *Sci. Rep.* **3,** 3476 (2013).
34. Yu, Y. F. *et al.* Optical-force-induced bistability in nanomachined ring resonator systems, *Appl. Phys. Lett.* **100,** 093108 (2012).
35. Kyriienko, O., Liew, T. C. H. & Shelykh, I. A. Optomechanics with Cavity Polaritons: Dissipative Coupling and Unconventional Bistability, *Phys. Rev. Lett.* **112,** 076402 (2014).
36. Jiang, C. *et al.* Controllable optical bistability based on photons and phonons in a two-mode optomechanical system, *Phys. Rev. A* **88,** 055801 (2013).
37. Hill, J. T. *et al.* Coherent optical wavelength conversion via cavity optomechanics *Nat. Commun.* **3,** 1196 (2012).
38. Zhang, J. M., Cui, F. C. Zhou, D. L., and Liu, W. M. Nonlinear dynamics of a cigar-shaped Bose-Einstein condensate in an optical cavity, *Phys. Rev. A* **79,** 033401 (2009).
39. Yang, S. *et al.* Controllable optical switch using a Bose-Einstein condensate in an optical cavity, *Phys. Rev. A* **83,** 053821 (2011).
40. Esteve, J. *et al.* Squeezing and entanglement in a BoseEinstein condensate, *Nature* **455,** 1216 (2008).
41. Brennecke, F. *et al.* Cavity QED with a BoseEinstein condensate, *Nature* **450,** 268 (2007).
42. Zhang, X. F. *et al.* Rydberg Polaritons in a Cavity: A Superradiant Solid, *Phys. Rev. Lett.* **110,** 090402 (2013).
43. Öttl, A. *et al.* Hybrid apparatus for Bose-Einstein condensation and cavity quantum electrodynamics: Single atom detection in quantum degenerate gases, *Rev. Sci. Instrum.* **77,** 063118 (2006).
44. Kippenberg, T. J. & Vahala, K. J. Cavity Opto-Mechanics, *Optics Express* **15,** 17172 (2007).
45. Law, C. K. Interaction between a moving mirror and radiation pressure: A Hamiltonian formulation, *Phys. Rev. A* **51,** 2537 (1995).
46. Gardiner, C. W. *Quantum Noise* (Berlin, Springer, 1991).
47. Paternostro, M. *et al.* Reconstructing the dynamics of a movable mirror in a detuned optical cavity, *New J. Phys.* **8,** 107 (2006).
48. Giovannetti, V. & Vitali, D. Phase-noise measurement in a cavity with a movable mirror undergoing quantum Brownian motion, *Phys. Rev. A* **63,** 023812 (2001).
49. Dalafi, A., Naderi, M. H., Soltanolkotabi, M. & Barzanjeh, Sh. Controllability of optical bistability, cooling and entanglement in hybrid cavity optomechanical systems by nonlinear atomatom interaction, *J. Phys. B: At. Mol. Opt. Phys.* **46,** 235502 (2013).
50. Hilborn, R. C. *Chaos and Nonlinear Dynamics*, 2nd ed. (Oxford University Press, New York, 1980).
51. Saif, F. Classical and quantum chaos in atom optics, *Phys. Rep.* **419,** 207 (2005).

Acknowledgements

This work was supported by the NKBRSFC under grants Nos. 2011CB921502, 2012CB821305, NSFC under grants Nos. 61227902, 61378017, 11434015, SKLQOQOD under grants No. KF201403, SPRPCAS under grants No. XDB01020300. We strongly acknowledge financial support from CAS-TWAS president's fellowship programme (2014).

Author Contributions

K.A.Y. and W.-M.L. proposed the ideas. K.A.Y. interpreted physics, performed the theoretical as well as the numerical calculations and wrote the main manuscript. W.-M.L. checked the calculations and the results. Both of the authors reviewed the manuscript.

Additional Information

Competing financial interests: The authors declare no competing financial interests.

How to cite this article: Yasir, K. A. and Liu, W.-M. Tunable Bistability in Hybrid Bose-Einstein Condensate Optomechanics. *Sci. Rep.* **5**, 10612; doi: 10.1038/srep10612 (2015).

This work is licensed under a Creative Commons Attribution 4.0 International License. The images or other third party material in this article are included in the article's Creative Commons license, unless indicated otherwise in the credit line; if the material is not included under the Creative Commons license, users will need to obtain permission from the license holder to reproduce the material. To view a copy of this license, visit http://creativecommons.org/licenses/by/4.0/